Contents lists available at ScienceDirect

Synthetic Metals

journal homepage: www.elsevier.com/locate/synmet

EPR monitoring of aniline polymerization: Kinetics and reaction mechanism

Y.O. Mezhuev [a,*], M.V. Motyakin [b,c], I.Yu. Vorobev [a], I.V. Plyushchii [a], A.L. Luss [a], I.S. Ionova [c], A.L. Kovarskii [b], Yu Cai [d,e], M.I. Shtilman [a], A.M. Tsatsakis [f], C. Zaharia [g], Yu.V. Korshak [a]

[a] Mendeleev University of Chemical Technology of Russia, 125047 Moscow, Russia
[b] Emanuel Institute of Biochemical Physics, Russian Academy of Sciences, 119334 Moscow, Russia
[c] Semenov Federal Research Center for Chemical Physics, Russian Academy of Sciences, 119991 Moscow, Russia
[d] College of Pharmacy, Jinan University, Guangzhou, Guangdong 510632, China
[e] Guangdong Key Lab of Traditional Chinese Medicine Information Technology, Guangzhou, Guangdong 510632, China
[f] Center of Toxicology Science & Research, Division of Morphology, Medical School, University of Crete, Voutes Campus, Heraklion 71003, Crete, Greece
[g] Politehnica University of Bucharest, Advanced Polymer Materials Group, 1-7 Gh. Polizu Street, Sector 1, 011061 Bucharest, Romania

ARTICLE INFO

ABSTRACT

The possibility of using EPR spectroscopy to monitor the current concentration of polyaniline and control the kinetics of aniline polymerization is shown. Kinetic measurements were carried out for various temperatures, initial concentrations of reagents. Autocatalysis was detected in all cases. It was shown that the order of polyaniline-catalyzed oxidation of aniline changes from the first to the second as a result of a decrease in the monomer concentration. A new approach to deriving an equation for the rate of oxidative polymerization of aniline and its derivatives is proposed taking into account the physical adsorption and chemisorption of the monomer, and the reaction mechanism is considered.

1. Introduction

The combination of significant electrical conductivity [1], high chemical and thermal stability [2–4] provided an increased interest in the study of synthesis, properties [5,6], directions of application of polyaniline and its derivatives [7–9]. The establishment of the mechanism and kinetics of polymerization is traditionally one of the important points in the search for relationships between the properties of macromolecules and the conditions of their synthesis. Although the mechanism of many classes of polymer synthesis reactions has been established, the nature of chain growth in oxidative polymerization is the subject of numerous discussions in literature [10]. Until recently even the nature of the active centers of the oxidative polymerization of aromatic amines was discussed, and the participation of radicals [11], cations [12–14], and radical cations [15–17] was considered as alternative options. The increased activity of monomers with electron-donor substituents in the oxidative polymerization of aniline derivatives indicates the formation of positively charged particles as intermediates [18,19]. Kinetic data [15–18], the absence of chain cross-linking [20] and the inefficiency of typical cationic "traps" in the interception of

intermediates [21] suggest that radical cations are active centers of oxidative polymerization of aniline derivatives.

It was found that the kinetics of oxidative polymerization of aromatic amines can be satisfactorily described by the kinetic Eq. (1) [15–18, 20–22].

$$-\frac{dC_M}{dt} = r_{nc} + r_c = k_{nc}C_M C_{Ox} + \sigma k_c C_M \left(C_M^0 - C_M \right) \tag{1}$$

where r_{nc}, r_c – rates of non-catalytic and catalytic oxidation of the monomer; k_{nc}, k_c – rate constants of non-catalytic and catalytic oxidation of the monomer; C_M, C_{Ox} – concentrations of monomer and oxidizing agent; σ – the surface factor [15]; t – time.

The first order rate of the catalytic step with respect to the concentrations of aniline and polyaniline, as well as its independence from the concentration of the oxidizing agent, made it possible to assume that the monomer is oxidized directly by the polymer (Scheme 1). Thus, it is assumed in [15] that the role of the oxidizing agent in the catalytic step belongs to the pernigraniline form, which is reduced to the emeraldine form. Reoxidation of the emeraldine form leads to the regeneration of

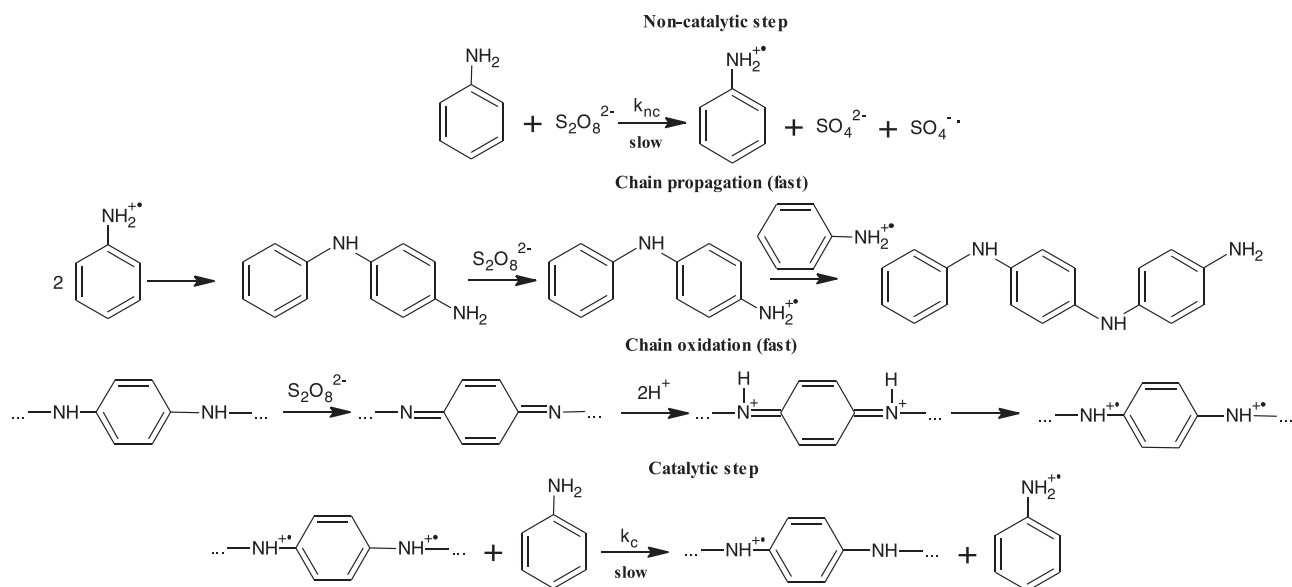**Scheme 1.** Mechanism of aniline polymerization explaining the autocatalytic course of the reaction by the oxidation of aniline with pernigraniline.

pernigraniline, closing the catalytic cycle. This mechanism is assumed to be common for the polymerization of aromatic amines under the action of various oxidizing agents [16–18].

Recent theoretical results indicate the impossibility of pernigraniline formation at low monomer conversion, although autocatalysis begins to manifest itself at an aromatic amine conversion of about 1% [23]. In addition, the intermediate formation of pernigraniline is not facilitated by its low hydrolytic stability in acidic aqueous solutions [24]. Apparently, the formation of pernigraniline is possible only at the final stage of the reaction. A careful analysis of the molecular weight distribution (MWD) of polyanilines shows the progress of the reaction of nucleophilic addition of the terminal primary amino group of aniline oligomer chains to quinone diimine fragments (chain branching) [25]. A similar process, all the more, should take place during the interaction of pernigraniline with aniline itself, leading to the nucleophilic addition of the latter, and not to its oxidation. These contradictions can be eliminated on the assumption that the polymer initially adsorbs the monomer, causing its polarization. Then the adsorbed polarized form of the monomer undergoes oxidation by the impact mechanism under the action of an oxidizing agent in an aqueous solution, as we proposed earlier [20,26].

Studying the kinetics of oxidative polymerization is a simple and representative approach to establish its mechanism, especially considering the variety of methods used to monitor the current concentrations of reagents and reaction products. For example, kinetic curves of polymerization of aromatic amines were obtained by gas chromatography [15], electron spectroscopy [27], Raman spectroscopy [28], ^{1}H NMR spectroscopy [16–18,22], calorimetry [29], potentiometry [30] and others methods [31–33]. It is noteworthy that although the paramagnetic properties of doped polyaniline are known and EPR has been intensively studied [34–37], this method has not previously been used to control the kinetics of precipitation polymerization of aromatic amines. Therefore, this article is devoted to the application of the EPR spectroscopy method to control the kinetics of aniline polymerization, to a quantitative examination of the obtained results, and to clarification of the details of the reaction mechanism.

2. Experimental

2.1. Materials and methods

Aniline hydrochloride (purity not less than 99%) and ammonium peroxodisulfate (purity not less than 98%) purchased from "Sigma –

Aldrich" were used as reagents. X-band EPR spectra were recorded on a commercial Bruker EMX spectrometer (Germany).

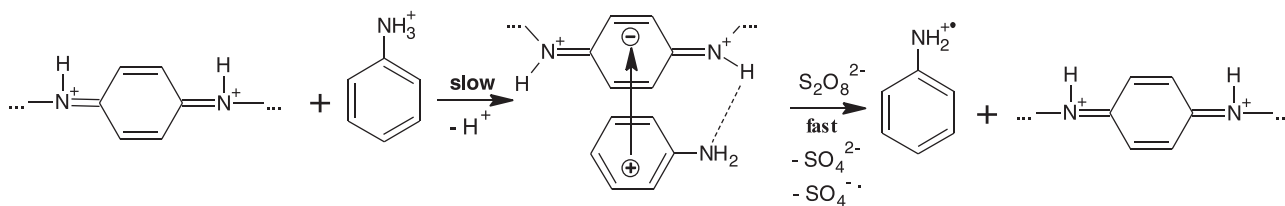### 2.2. Study of the kinetics of aniline polymerization

Solutions with concentrations of 0.2 M, 0.1 M, and 0.05 M were prepared by dissolving aniline hydrochloride in 50 ml of distilled water. Solutions with concentrations of 0.25 M, 0.125 M, and 6.25×10^{-2} M were prepared by dissolving $(NH_4)_2S_2O_8$ in 50 ml of distilled water. After thermostating until the desired temperature was established, aliquots of the solutions were mixed so that the excess of $(NH_4)_2S_2O_8$ with respect to the monomer was 1.25. The reaction was carried out at temperatures of 284 K, 294 K, and 304 K in the resonator of an EPR spectrometer, recording the values of the signal intensity. The EPR spectrometer operates at 9.8 GHz and 100 KHz magnetic field modulation and is equipped with a variable temperature unit. The samples were placed into a resonator of the spectrometer using 0.9 mm id Bruker glass capillaries. The following parameters were used for spectral acquisition: microwave power 2 mW; sweep width 70 G; conversion time 40.96 ms; time constant 40.96 ms; modulation amplitude 0.7 G; number of points 1024. As it was checked, the modulation value of 0.7 G does not affect the shape and width of the detected signal, which caused the choice of this value. Mathematical processing of the EPR spectra, in particular, double integration, was carried out using the WINEPR and SIMFONIA (Bruker) programs. The error in determining the position of the experimental points in time is up to 15 s. The error was minimized by computer processing of signals after the registration of all spectra was completed. The values of the integral signal intensities were related to the recording time when the signal center passed.

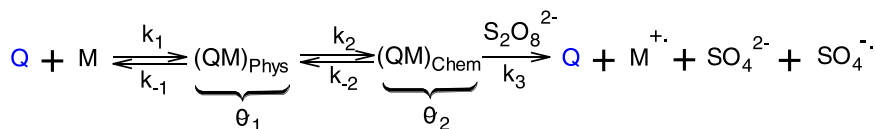The current concentration of monomer was calculated according to the Eq. (2):

$$C_M = C_M^0 \left(1 - \frac{I}{I_\infty} \right) \tag{2}$$

where I, I_∞ - current and maximum value of the integrated intensity of the polyaniline signal in the EPR spectrum. The derivation of Eq. (2) is given in the "Supplementary Data" section.

The selected conditions for the oxidative polymerization of aniline make it possible to monitor the reaction kinetics for a time not exceeding 200 min, and also to vary the temperature in a range representative for determining the activation energy.

Scheme 2. The mechanism of autocatalysis of aniline polymerization, assuming the polarization of the monomer with polyaniline.

$$Q + M \underset{k_{-1}}{\overset{k_1}{\rightleftharpoons}} \underbrace{(QM)_{Phys}}_{\theta_1} \underset{k_{-2}}{\overset{k_2}{\rightleftharpoons}} \underbrace{(QM)_{Chem}}_{\theta_2} \overset{S_2O_8^{2-}}{\underset{k_3}{\longrightarrow}} Q + M^{+\cdot} + SO_4^{2-} + SO_4^{-\cdot}$$

Scheme 3. Kinetic scheme explaining the effect of autocatalysis during oxidative polymerization (Q - quinone diimine fragments of polyaniline; $(QM)_{Phys}$ - physically adsorbed aniline; $(QM)_{Chem}$ - chemisorbed aniline; M, $M^{+\cdot}$ - aniline and aniline radical cation.

3. Results and discussion

3.1. Theoretical consideration of the kinetics and mechanism of oxidative polymerization of aniline derivatives

It is known that the rate of monomer oxidation catalyzed by polyaniline does not decrease with an increase in the acidity of the medium; therefore, the salt form is active in this act, but not the basic form of aniline [15]. Therefore, the following mechanism of the catalytic stage can be assumed, including the induced dissociation of the phenylammonium cation (Scheme 2). The driving force of the induced dissociation, most likely, is the minimization of electrostatic repulsion when the positively charged polyaniline chain and the phenylammonium cation approach each other, as well as the possibility of hydrogen bonding (Scheme 2).

Since polyaniline simultaneously catalyzes the oxidative polymerization of aniline and forms a new phase [15–18,20–22], the adsorption of aniline on polyaniline is the most important process that largely determines the nature of the kinetic relationships [20,26]. Let us denote by θ_∞ the total surface concentration of all adsorption centers of doped polyaniline. In the general case, both physical and chemical adsorption of an aromatic amine is possible, and there is an equilibrium between the two states of the adsorbate. Let θ_1 and θ_2 be the surface concentrations of a physically adsorbed and chemisorbed aromatic amine, respectively. Thus, when considering the kinetics of the catalytic action of polyaniline, Scheme 3 is adopted.

Taking the principle of stationarity with respect to surface concentrations of physically adsorbed and chemisorbed aromatic amine, we write Eqs. (3) and (4):

$$\frac{d\theta_1}{dt} = k_1(\theta_\infty - \theta_1 - \theta_2)C_M + k_{-2}\theta_2 - (k_{-1}+k_2)\theta_1 = 0 \quad (3)$$

$$\frac{d\theta_2}{dt} = k_2\theta_1 - k_{-2}\theta_2 - k_3\theta_2 C_{Ox} = 0 \quad (4)$$

where C_M, C_{Ox} - concentration of monomer and oxidizing agent; θ_∞ - total surface concentration of all adsorption centers of polyaniline; θ_1 and θ_2 are surface concentrations of physically adsorbed and chemisorbed aromatic amine, respectively; $k_1, k_{-1}, k_2, k_{-2}, k_3$ - the rate constants explained by Scheme 3.

Solving the system of algebraic Eqs. (3) and (4), we obtain the Eq. (5) for θ_2:

$$\theta_2 = \frac{k_1 k_2 \theta_\infty C_M}{k_{-1}k_{-2} + k_1 C_M(k_2+k_{-2}) + k_3(k_1 C_M + k_{-1} + k_2)C_{Ox}} \quad (5)$$

Thus, the rate of polymer-catalyzed oxidation of the monomer can be written in the form of the Eq. (6):

$$r_c = k_3\theta_2 C_{Ox}s = \frac{k_1 k_2 k_3 \theta_\infty C_M C_{Ox}s}{k_{-1}k_{-2} + k_1 C_M(k_2+k_{-2}) + k_3(k_1 C_M + k_{-1} + k_2)C_{Ox}} \quad (6)$$

where s is the area of the interface per unit volume of the reaction system.

Considering the polymerization rate during the induction period ($r_{nc} = k_{nc}C_M C_{Ox}$), we write the Eq. (7):

$$-\frac{dC_M}{dt} = k_{nc}C_M C_{Ox} + \frac{k_1 k_2 k_3 \theta_\infty C_M C_{Ox}s}{k_{-1}k_{-2} + k_1 C_M(k_2+k_{-2}) + k_3(k_1 C_M + k_{-1} + k_2)C_{Ox}} \quad (7)$$

Obviously, the value of s depends on the conversion of the monomer and the average radius of the particles formed by the polymer, in accordance with Eq. (8) ("Supplementary Data"):

$$s = \frac{3M_M}{d_P \overline{R}}\left(C_M^0 - C_M\right) = \varepsilon\left(C_M^0 - C_M\right) \quad (8)$$

where M_M is the molecular weight of the aromatic amine; d_P is the density of the polymer; $\overline{R}$ is the average radius of the particles formed as a result of polymerization; $\varepsilon = \frac{3M_M}{d_P \overline{R}}$ is a constant depending on the structural features and sizes of the resulting polymer particles.

After substituting (8) into (7), we obtain (9).

$$-\frac{dC_M}{dt} = k_{nc}C_M C_{Ox} + \frac{k_1 k_2 k_3 \varepsilon \theta_\infty C_M \left(C_M^0 - C_M\right)C_{Ox}}{k_{-1}k_{-2} + k_1 C_M(k_2+k_{-2}) + k_3(k_1 C_M + k_{-1} + k_2)C_{Ox}} \quad (9)$$

Since the experimental kinetic data indicate that the rate of catalytic oxidation of an aromatic amine is independent of the oxidant concentration [15–17], the values of k_2 and k_{-2}, should be small. The latter means limiting the rate of the catalyzed oxidation of the aromatic amine by the practically irreversible slow formation of the chemisorbed form of the aromatic amine. Thus, we can write down the final kinetic Eq. (10):

$$-\frac{dC_M}{dt} = k_{nc}C_M C_{Ox} + \frac{K_M k_2 \varepsilon \theta_\infty \left(C_M^0 - C_M\right)C_M}{K_M C_M + 1} \quad (10)$$

where $K_M = \frac{k_1}{k_{-1}}$ is the adsorption equilibrium constant for an aromatic amine. Details of transformation (9) into Eq. (10) are given in the "Supplementary Data" section.

Comparison of Eq. (10) with the previously established experimentally Eq. (1) allows one to give a theoretical expression (11) for the parameter σ.

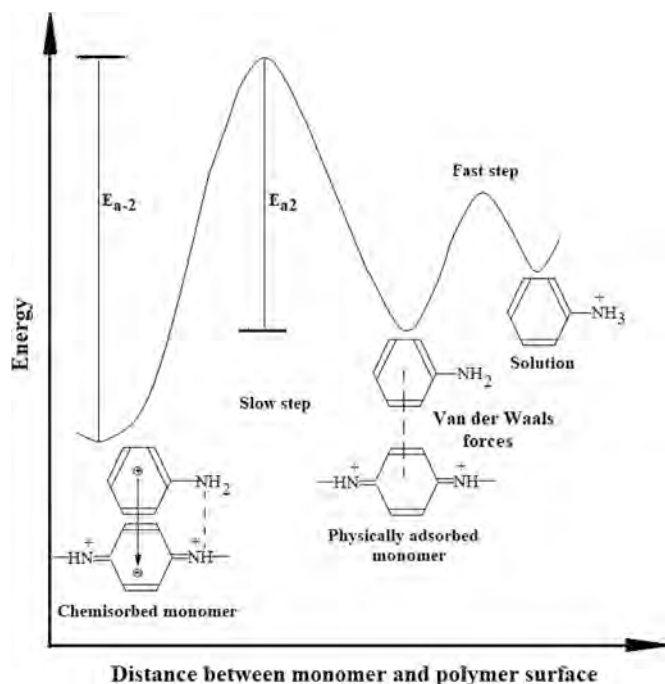$$\sigma = \frac{K_M \varepsilon \theta_\infty}{K_M C_M + 1} \quad (11)$$

Fig. 1. Estimated energy diagram of the adsorption of aniline on the surface of polyaniline.

As can be seen, the parameter σ depends not only on the surface properties, which determine the value of θ_∞, but also on the size of the resulting polymer particles and the concentration of the aromatic amine. The dependence of σ on the aromatic amine concentration means the possibility of changing the general order of the rate of polymer-catalyzed monomer oxidation. Although there are no data on the structure of adsorption layers formed on the surface of the polymer during oxidative polymerization, it is possible to assume the formation of complexes stabilized by charge transfer and hydrogen bonds as a result of chemisorption (Fig. 1). The preceding chemisorption, physical adsorption of the monomer can be associated with the action of Van der Waals forces.

The charge transfer and the formation of hydrogen bonds between the aromatic amine and the resulting polymer, first, is indirectly consistent with the strong association of chains in polyaniline solutions, which decreases upon going from the emeraldine form to the leucoemeraldine form [38]. Second, aromatic amines containing electron-withdrawing nitro groups do not homopolymerize [39,40]; however, the introduction of even a small amount of aniline ensures their involvement in copolymerization [41]. Apparently, even amines with electron-withdrawing substituents behave as donors in the presence of electron-deficient doped polyaniline chains [20]. The inability to homopolymerize aromatic amines with electron-withdrawing substituents is probably a consequence of their passivity in oxidation uncatalyzed by the polymer (induction period); however, this does not exclude their catalytic oxidation upon the introduction of a second monomer capable of forming a seed amount of polymer. Finally, it is known that some aromatic compounds containing simultaneously donor amino groups and acceptor quinone diimine fragments form stable dimers structurally similar to quinhydrone [42–44]. An example of such a compound is the dye methylene blue [45]. In addition, the structures of adsorbates shown in Fig. 1 make it possible to qualitatively explain the presence of a significant activation barrier between the physically adsorbed and chemisorbed monomer. The reason for the significant activation barrier is the electrostatic repulsion of the monomer, which acquires a positive charge as a result of binding into a complex (Scheme 2), from the side of the positively charged chain of the doped polyaniline.

3.2. Integration of the kinetic equation for the oxidative polymerization of aniline derivatives

To compare the experimental data and theoretical results, as well as to determine the kinetic constants, Eq. (10) must be integrated. Exact integration (10) leads to a complex transcendental function with respect to the rate constants, which complicates their determination. However, Eq. (10) is greatly simplified if we assume a low degree of filling of the polymer surface with an aromatic amine or, on the contrary, the realization of conditions close to adsorption saturation (see section "Supplementary Data"). If the degree of filling the polyaniline surface with monomer is small, then (10) turns into (12), which is similar to the previously experimentally established Eq. (1) [15].

$$-\frac{dC_M}{dt} = k_{nc}C_M C_{Ox} + k_2'\left(C_M^0 - C_M\right)C_M \tag{12}$$

where $k_2' = K_M k_2 \varepsilon \theta_\infty$.

Integration (12) is described in articles [15–18], and leads to Eq. (13):

$$C_M = \frac{C_M^0 \beta_2}{C_M^0 \beta_1(\exp(\beta_2 t) - 1) + \beta_2 \exp(\beta_2 t)} \tag{13}$$

where $\beta_1 = 1.25 k_{nc} - k_2'$ и $\beta_2 = k_{nc}C_{Ox}^0 - \beta_1 C_M^0$; C_{Ox}^0 – initial concentration of oxidizing agent.

In the case of realization of conditions close to adsorption saturation, from (10) we obtain (14):

$$-\frac{dC_M}{dt} = k_{nc}C_M C_{Ox} + k''_2\left(C_M^0 - C_M\right) \tag{14}$$

where $k_2'' = k_2 \varepsilon \theta_\infty$.

Integration (14) leads to (15):

$$C_M = \frac{(b+\lambda)\exp(-\lambda t) - \varphi(b-\lambda)}{2.5 k_{nc}(\varphi - \exp(-\lambda t))} \tag{15}$$

where $b = k_{nc}C_{Ox}^0 - 1.25 k_{nc}C_M^0 - k_2''$; $\lambda = (b^2 - 5k_{nc}k_2''C_M^0)^{0.5}$;

$$\varphi = \frac{2.5 k_{nc}C_M^0 + b + \lambda}{2.5 k_{nc}C_M^0 + b - \lambda}$$

As can be seen, Eqs. (13) and (15) are transcendental with respect to the parameters included in them, but they can be used to approximate experimental data by the "fitted curve" method, which makes it possible to estimate the constants. If the values k_2' 'and k_2'' can be calculated with significant accuracy, then the error in determining k_{nc} by the "fitted curve" method is large, as noted earlier [22].

Apparently, there is no need to obtain exact integrals of differential Eqs. (12) and (14) to achieve a satisfactory mathematical description of the kinetic curves. As a convenient approximation, it can be taken that the rate of the noncatalytic stage does not depend on the conversion of the monomer and oxidant during the induction period, and after its completion it is equal to zero (much less than the rate of the autocatalytic stage) [26]. This approximation leads to Eqs. (16) and (17), which make it possible to determine the constants k_2' and k_2'' without resorting to the "fitted curve" method by the slopes of the dependences $\ln\{(C_M^0 - C_M)C_M^{-1}\}$ vs t and $\ln(C_M^0 - C_M)$ vs t, respectively. However, the determination of the constant k_{nc}, obviously, will also be associated with a significant error.

$$\ln\{(C_M^0 - C_M)C_M^{-1}\} = \xi' + k_2'C_M^0 t \tag{16}$$

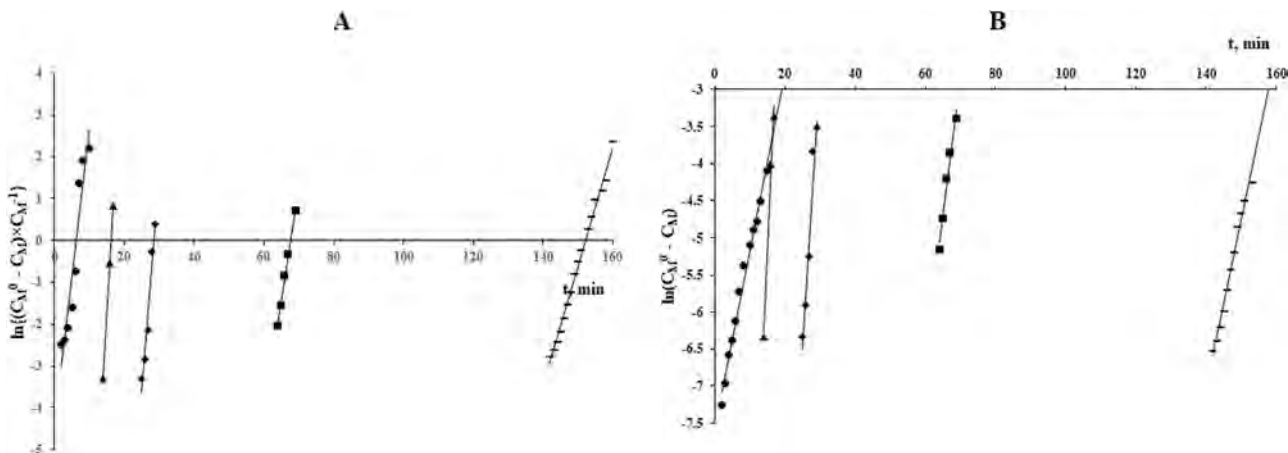$$\ln(C_M^0 - C_M) = \xi'' + k_2'' t \tag{17}$$

Fig. 2. Dependence $\ln\{(C_M^0 - C_M)C_M^{-1}\}$ vs t – A и $\ln(C_M^0 - C_M)$ vs t – B (segments ($C_M^0 = 0.025M$, T = 284 K); squares ($C_M^0 = 0.05M$, T = 284 K); rounds ($C_M^0 = 0.1M$, T = 284 K); rhombuses ($C_M^0 = 0.05M$, T = 294 K); triangles ($C_M^0 = 0.05M$, T = 304 K).

where $\xi' = ln\left|\dfrac{k_2'C_M^0 - \sqrt{4r_{nc}k_2' + (k_2'C_M^0)^2}}{k_2'C_M^0 + \sqrt{4r_{nc}k_2' + (k_2'C_M^0)^2}}\right|$ and $\xi'' = ln\left|\dfrac{r_{nc}}{k_2'}\right|$.

Therefore, to calculate k_{nc} the Eq. (18) was used.

$$k_{nc} = -\frac{\left(\frac{dC_M}{dt}\right)_{t=0}}{C_M C_{Ox}} \qquad (18)$$

The value $\left(\frac{dC_M}{dt}\right)_{t=0}$ is determined graphically from the tangent of the slope of the kinetic curve C_M vs t. A detailed discussion of the influence of the acidity of the medium on the rate of non-catalytic oxidation of aniline is given in "Supplementary Data".

The analysis of experimental data using Eqs. (16) and (17) should be carried out in the range of aniline conversion from 5% to 10% to 75–80%, since during the induction period and at the final stages of polymerization, the principle of stationarity underlying derivation of Eq. (10). The obtained experimental kinetic data form straight lines in co-ordinates $\ln\{(C_M^0 - C_M)C_M^{-1}\}$ vs t (Fig. 2A) and $\ln(C_M^0 - C_M)$ vs t

(Fig. 2B).

As can be seen (Fig. 2), high concentrations of aniline and low temperatures favoring adsorption saturation also contribute to the linearity of the kinetic curves in coordinates $\ln(C_M^0 - C_M)$ vs t. On the contrary, low concentrations of aniline and an increase in temperature lead to a straightening of the kinetic curves in coordinates $\ln\{(C_M^0 - C_M)C_M^{-1}\}$ vs t. These circumstances are consistent with the assumption of the important role of the adsorption of aniline on polyaniline, as well as the possibility of oxidative polymerization of aniline in frozen reaction mixtures [46].

3.3. EPR spectra of polyaniline and registration of the kinetics of aniline polymerization

It is known that the polymerization of aniline is accompanied by the appearance of an EPR signal associated with the formation of doped polyaniline [47,48]. The polaron model is widely used to explain the nature of paramagnetism of polyconjugated systems [49]. The dynamics of the appearance of polarons during the polymerization of aniline is typical for processes characterized by autoacceleration: an induction
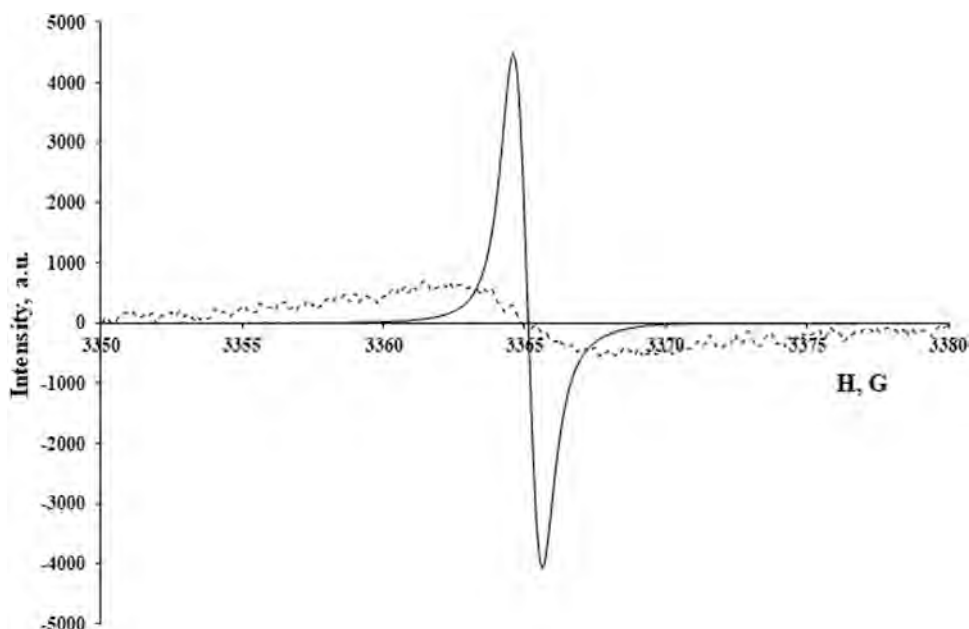

Fig. 3. EPR signals of polarons arising during the induction period (dashed line) and final stage (continuous line) of aniline polymerization at a temperature of 284 K.
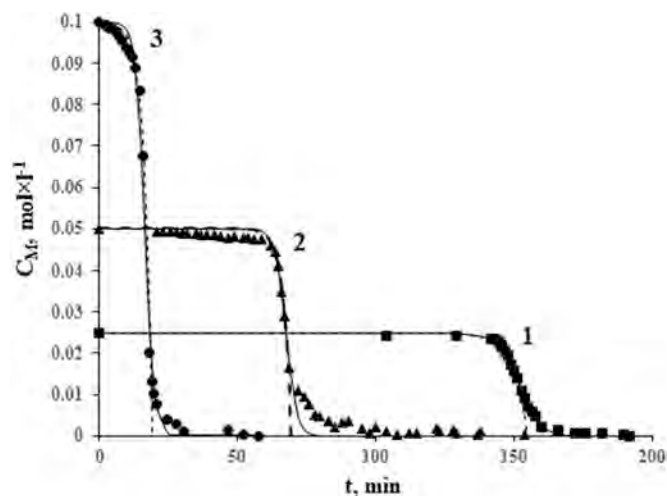
Fig. 4. Experimental dependences C_M vs t at a temperature of 284 K for various C_M^0: 1 – 0.025M; 2 – 0.05M; 3 – 0.1M ($C_{Ox}^0 = 1.25 C_M^0$; points - experimental data; continuous line corresponds to Eq. (19); dashed line corresponds to Eq. (20)).

period, a sharp increase in concentration followed by reaching maximum value. The EPR signal of polarons during the induction period is a symmetric singlet of the Lorentzian line shape with a width of $\Delta H = 7.4 \pm 0.1$ G and $g = 2.0030 \pm 0.0001$, which, with the polymerization time, transforms into a singlet of the Lorentzian line shape with a width of $\Delta H = 1.1 \pm 0.1$ G and $g = 2.0030 \pm 0.0001$ (Fig. 3).

The change in the signal width coincides with the onset of a sharp increase in the concentration of polarons, which is associated with an increase in the length of conjugated chains in proportion to the conversion of aniline [23]. A similar regularity in the change in the width of the EPR signal line during the polymerization of aniline was also noted in [50]. The described regularities of changes in the width and intensity of the polaron signal are the same for all investigated reagent concentrations and temperatures.

Retention of the width of the EPR signal up to deep conversions of aniline after its decrease at the end of the induction period makes it possible to use Eq. (2) to monitor the kinetics of polymerization. In connection with the above, the kinetic approach based on the independent determination of the rate constant k_{nc} from the EPR data in accordance with Eq. (18) is quite reasonable. Thus, the control of the kinetics of oxidative polymerization by the EPR method does not require stopping the reaction and the release of products; it makes it possible to quickly monitor the concentration of polymer and monomer and makes it possible to accurately determine the moment of completion of the induction period. As will be shown below, the rate constants determined by the EPR method agree with their values calculated as a result of monitoring the current concentration of aniline by ^{1}H NMR spectroscopy [22].

3.4. Change of order in the concentration of aniline

The derived kinetic Eq. (10) differs from the previously experimentally established kinetic Eq. (1) by the possibility of realizing the first order autocatalytic stage under conditions close to adsorption
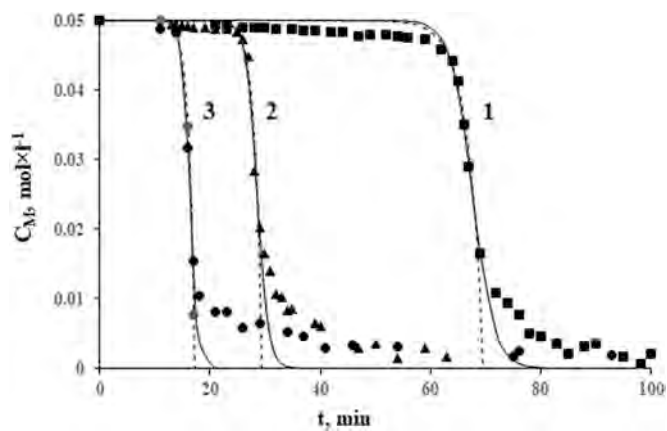

Fig. 5. Experimental dependences C_M vs t at temperatures: 1–284 K; 2–294 K; 3–304 K ($C_M^0 = 0.05$M; $C_{Ox}^0 = 0.0625$M; points - experimental data; continuous line corresponds to Eq. (19); dashed line corresponds to Eq. (20)).

saturation. Therefore, kinetic studies of oxidative polymerization in solutions with different initial concentrations of aniline hydrochloride were carried out while maintaining a 1.25-fold excess of $(NH_4)_2S_2O_8$ and a constant temperature of 284 K.

As a first approximation, the constants k_2' and k_2'', as well as ξ' and ξ'', were determined from the slope coefficients of the dependences $\ln\left\{(C_M^0 - C_M)C_M^{-1}\right\}$ vs t and $\ln\left(C_M^0 - C_M\right)$ vs t (Fig. 2), and then their values were refined by approximating the experimental kinetic curves by Eqs. (19) and (20) obtained by resolving (16) and (17) with respect to C_M.

$$C_M = \frac{C_M^0}{1 + \exp[f_0](\xi' + k_2' C_M^0 t)} \tag{19}$$

$$C_M = C_M^0 - \exp[f_0](\xi'' + k_2'' t) \tag{20}$$

Eqs. (19) and (20) turned out to be satisfactory for describing the experimental dependences (Fig. 4).

The values k_2', k_2'', ξ' and ξ'' used for the mathematical description of the experimental data, as well as the values of k_{nc} calculated by Eq. (18), are presented in Table 1.

Despite the formal satisfactory correspondence of theoretical Eqs. (19) and (20) to the kinetic curves (Fig. 4), the constants k_2' и k_2'' should not significantly depend on the concentration of aniline, if the order in terms of the concentration of the monomer for the rate of the autocatalytic stage remains constant. Taking into account the latter circumstance, the data in Table 1 indicate the realization of conditions close to adsorption saturation at a monomer concentration of about 0.1 M. On the contrary, far from adsorption saturation, kinetic Eqs. (1) and (19) are satisfied. Thus, the second order of catalytic oxidation of aniline is facilitated by its low concentration in the system, which corresponds to Eq. (10). The nature of the deviation of the theoretical dependences from the experimental data (Fig. 3) shows that Eq. (20), which is applicable under conditions of adsorption saturation, is always inadequate in the region of high conversions (low concentrations) of the monomer, but better agrees with the experimental data in the region of high aniline concentrations. On the contrary, Eq. (19) corresponds to the

Table 1
Parameters of kinetic Eqs. (19) and (20) at a temperature of 284 K.

C_M^0 mol $\times$ l^{-1}	k_2' $l \times mol^{-1} \times min^{-1}$	k_2'' min^{-1}	ξ'	ξ''	k_{nc} $l \times mol^{-1} \times min^{-1}$
0.1	6.0	0.37	-9.95	-9.38	0.013
0.05	10.2	0.36	-34.50	-27.94	
0.025	11.4	0.23	-43.52	-38.84	

Table 2

Parameters of kinetic Eqs. (19) and (20) for different temperatures of aniline polymerization ($C_M^0 = 0.05M$; $C_{Ox}^0 = 0.0625M$).

T K	k_2' $l \times mol^{-1} \times min^{-1}$	k_2'' min^{-1}	ξ'	ξ''	k_{nc} $l \times mol^{-1} \times min^{-1}$
284	10.2	0.36	-34.50	-27.94	0.013
294	19.6	0.77	-28.00	-25.79	0.021
304	29.2	1.02	-23.94	-20.51	0.047
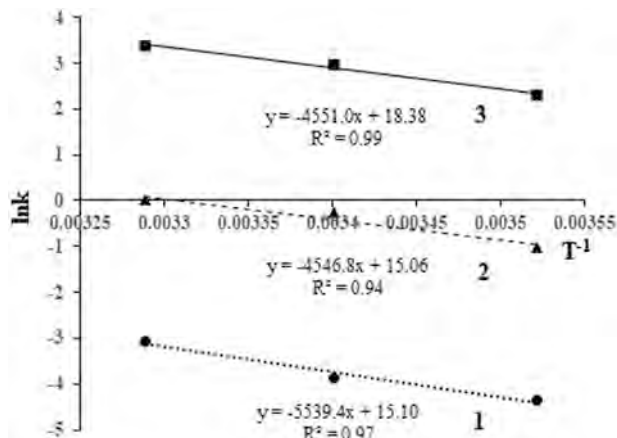
Fig. 6. Temperature dependences of rate constants: 1- k_{nc}; 2 - k_2''; 3 - k_2'.

experimental data obtained at an initial concentration of 0.025 M aniline.

Thus, the change in the order of the stage of catalytic oxidation of aniline is consistent with Eq. (10), which underlies the quantitative analysis of the kinetics. At the same time, kinetic Eq. (1) does not explicitly imply a change in the order of the catalytic oxidation stage. However, this effect can also be taken into account by Eq. (1) if it is assumed that the surface factor depends on the concentration of the monomer, in accordance with the previously derived Eq. (11).

3.5. Effect of temperature on the rate of polymerization of aniline

Eqs. (19) and (20) are in satisfactory agreement with the kinetic data obtained for different temperatures of polymerization (Fig. 5).

The algorithm described above makes it possible to determine k_2', k_2'', ξ' and ξ'' for different temperatures of aniline polymerization (Table 2).

The results obtained indicate an increase in the rate of polymerization of aniline with increasing temperature. The rate constant k_{nc} increases faster than k_2' and k_2'' as the temperature rises. The activation energy of the reaction during the induction period is about 46 kJ $\times$ mol^{-1}, whereas for the stage catalyzed by polyaniline, its value is 37.5 kJ $\times$ mol^{-1} and is practically independent of the kinetic order assumption (Fig. 6). Thus, the obtained kinetic data confirm that the autoacceleration of the oxidative polymerization of aniline is a consequence of autocatalysis. The assumption about the implementation of the second order stage of catalytic oxidation of the monomer leads to a better agreement between theoretical and experimental data at all studied temperatures (Fig. 5), and provides a larger value of R^2 for the dependence $lnk_1 = f(T^{-1})$ (Fig. 6).

The obtained kinetic data indicate the absence of a pronounced dependence of the constants k_2'', k_2' on the particle size of the resulting polyaniline, otherwise these values would change significantly with the conversion of the monomer. Possible reasons for the independence of

the rate constants of the catalyzed oxidation of aniline on the size of the resulting polyaniline particles were considered earlier [23].

Finally, the catalytic component of the rate of oxidative polymerization in Eq. (10) is derived in a stationary approximation, which cannot be fulfilled at both low and high monomer conversions. At low conversions of the monomer, violation of the principle of stationarity does not affect the results of kinetic calculations according to Eq. (10) (Fig. 4 and Fig. 5), since $C_M \approx C_M^0$ and the contribution of the catalytic component of the rate to the total rate of oxidative polymerization of aniline is insignificant. As shown in Figs. 4 and 5, when the conversion of aniline is more than 80%, the kinetic model in all cases becomes inadequate, which is a consequence of the violation of the principle of stationarity. Thus, Eq. (10) is fulfilled until deep monomer conversions of 75–80% are achieved. Apparently, the kinetic Eq. (10) is valid only for the oxidation of aniline and its derivatives in strongly acidic media. Other assumptions, associated with the need to integrate Eq. (10) suggest considering only the cases of adsorption saturation or, on the contrary, the formation of rarefied adsorption layers of the monomer on the polyaniline surface. At the same time, in all kinetic calculations, the rate of the monomer oxidation stage uncatalyzed by polyaniline is assumed to be constant and significant only during the induction period.

4. Conclusion

EPR spectroscopy is a convenient method of kinetic measurements for the oxidative polymerization of aniline. The change in the EPR spectrum on going from aniline oligomers to polyaniline, which coincides with the onset of the autocatalytic acceleration of polymerization, makes it possible to determine the duration of the induction period. It is shown that the chemisorption of aniline on polyaniline determines the degree of surface coverage and the kinetic order of the stage of monomer oxidation catalyzed by polyaniline. For the first time, a theoretical expression for the surface factor was given and it was found that it depends not only on the surface properties and the size of polymer particles, but also on the monomer concentration. It has been suggested that the chemisorption of the monomer is a stage that limits the rate of oxidative polymerization of aromatic amines after the end of the induction period.

CRediT authorship contribution statement

Declaration of Competing Interest

The authors declare that they have no known competing financial interests or personal relationships that could have appeared to influence the work reported in this paper.

Acknowledgements

Funding

Appendix A. Supporting information

Supplementary data associated with this article can be found in the online version at doi:10.1016/j.synthmet.2021.116871.

References

[1] T.-H. Le, Y. Kim, H. Yoon, Electrical and electrochemical properties of conducting polymers, Polymers 9 (12) (2017) 150, https://doi.org/10.3390/polym9040150.
[2] Vaman G. Kulkarni, Larry D. Campbell, William R. Mathew, Thermal stability of polyaniline, Synth. Met. 30 (3) (1989) 321–325, https://doi.org/10.1016/0379-6779(89)90654-1.
[3] Libuše Brožová, Petr Holler, Jana Kovářová, Jaroslav Stejskal, Miroslava Trchová, The stability of polyaniline in strongly alkaline or acidic aqueous media, Polym. Degrad. Stabil. 93 (3) (2008) 592–600, https://doi.org/10.1016/j.polymdegradstab.2008.01.012.
[4] Stephen C. Hobaica, Stability of polyaniline in air and acidic water, J. Polym. Sci. Part B 41 (8) (2003) 807–822, https://doi.org/10.1002/polb.10437.
[5] P. Fedorko, J. Faure-Vincent, I. Fier, L. Walmsley, M. Sniechowski, J.F. Jacquot, A. Pron, J.P. Travers, D. Djurado, Effect of structural anisotropy on electrical and magnetic properties of polyaniline conducting films, Synth. Met. 166 (2013) 63–69, https://doi.org/10.1016/j.synthmet.2013.01.017.
[6] Tomasz Kozik, Maciej Śniechowski, Wojciech Łużny, Adam Proń, David Djurado, Neutron diffraction study of conducting polyaniline doped with (±) camphorsulfonic acid, Polymer 111 (2017) 148–155, https://doi.org/10.1016/j.polymer.2017.01.034.
[7] X. Li, Preparation, properties and application of polyaniline nanocomposites, Chem. Eng. Trans. 71 (2018) 889–894, https://doi.org/10.3303/CET1871149.
[8] Effat Eskandari, Mohammadreza Kosari, Mohammad Hossein Davood Abadi Farahani, Negar Dasineh Khiavi, Mohsen Saeeidikhani, Reza Katal, Mehrdad Zarinejad, A review on polyaniline-based materials applications in heavy metals removal and catalytic processes, Sep. Purif. Technol. 231 (2020), 115901, https://doi.org/10.1016/j.seppur.2019.115901.
[9] T.K. Das, S. Prusty, Review on conducting polymers and their applications, Polym. Plast. Technol. Eng. 51 (14) (2012) 1487–1500, https://doi.org/10.1080/03602559.2012.710697.
[10] Irina Sapurina, Andrey V. Tenkovtsev, Jaroslav Stejskal, Conjugated polyaniline as a result of the benzidine rearrangement, Polym. Int. 64 (4) (2015) 453–465, https://doi.org/10.1002/pi.4869.
[11] H. Minami, M. Okubo, K. Murakami, S. Hirano, Kinetics of chemical oxidative dispersion polymerization of 3,5-xylidine in aqueous medium using a PH stat method, J. Polym. Sci. A Polym. Chem. 38 (2000) 4238–4246, https://doi.org/10.1002/1099-0518(20001201)38:23<4238::AID-POLA90>3.0.CO;2-2.
[12] Y. Wei, Y. Sun, X. Tang, Autoacceleration and kinetics of electrochemical polymerization of aniline, J. Phys. Chem. 93 (1989) 4878–4881, https://doi.org/10.1021/j100349a039.
[13] N. Gospodinova, L. Terlemezyan, Conducting polymers prepared by oxidative polymerization: polyaniline, Prog. Polym. Sci. 23 (1998) 1443–1484, https://doi.org/10.1016/S0079-6700(98)00008-2.
[14] X.X. Liu, L. Zhang, Y.-B. Li, L.-J. Bian, Y.-Q. Hio, Z. Su, Electrosynthesis of polyaniline/SiO₂ composite at high pH in the absence of extra supporting electrolyte, Polym. Bull. 57 (2006) 825–832, https://doi.org/10.1007/s00289-006-0653-9.
[15] K. Tzou, R.V. Gregory, Kinetic study of the chemical polymerization of aniline in aqueous solutions, Synth. Met. 47 (3) (1992) 267–277, https://doi.org/10.1016/0379-6779(92)90367-r.
[16] Ida Mav, Majda Žigon, ¹H NMR study of the kinetics of substituted aniline polymerization. I. Homopolymerization of 2-methoxyaniline, J. Polym. Sci. Part A 39 (14) (2001) 2471–2481, https://doi.org/10.1002/pola.1224.
[17] Ida Mav, Majda Žigon, ¹H NMR study of the kinetics of substituted aniline polymerization. II. Copolymerization of 2-methoxyaniline and 3-aminobenzene-sulfonic acid, J. Polym. Sci. Part A 39 (14) (2001) 2482–2493, https://doi.org/10.1002/pola.1225.
[18] I. Mav, M. Zigon, Chemical copolymerization of aniline derivatives: preparation of fully substituted PANI, Synth. Met. 119 (1–3) (2001) 145–146, https://doi.org/10.1016/s0379-6779(00)01289-3.
[19] Y. Wei, R. Hariharan, S.A. Patel, Chemical and electrochemical copolymerization of aniline with alkyl ring-substituted anilines, Macromolecules 23 (3) (1990) 758–764, https://doi.org/10.1021/ma00205a011.
[20] Ya.O. Mezhuev, Yu.V. Korshak, M.I. Shtilman, Oxidative polymerization of aromatic amines: kinetic features and possible mechanisms, Russ. Chem. Rev. 86 (12) (2017) 1271–1285, https://doi.org/10.1070/RCR4755.
[21] I. Yu Sapurina, Jaroslav Stejskal, The effect of pH on the oxidative polymerization of aniline and the morphology and properties of products, Russ. Chem. Rev. 79 (12) (2010) 1123–1143, https://doi.org/10.1070/RC2010v079n12ABEH004140.
[22] M.T. Gill, S.E. Chapman, C.L. DeArmitt, F.L. Baines, C.M. Dadswell, J.G. Stamper, G.A. Lawless, N.C. Billingham, S.P. Armes, A study of the kinetics of polymerization of aniline using proton NMR spectroscopy, Synth. Met. 93 (1998) 227–233, https://doi.org/10.1016/s0379-6779(98)00016-2.
[23] Yaroslav O. Mezhuev, Yuri V. Korshak, Theory of chain growth in chemical oxidative polymerization of aniline derivatives, Synth. Met. 267 (2020), 116445, https://doi.org/10.1016/j.synthmet.2020.116445.
[24] Yan Sun, Alan G. MacDiarmid, Arthur J. Epstein, Polyaniline: synthesis and characterization of pernigraniline base, J. Chem. Soc. Chem. Commun. 7 (1990) 529–531, https://doi.org/10.1039/c39900000529.
[25] Yen Wei, Kesyin F. Hsueh, Guang Way Jang, A study of leucoemeraldine and effect of redox reactions on molecular weight of chemically prepared polyaniline, Macromolecules 27 (2) (1994) 518–525, https://doi.org/10.1021/ma00080a028.
[26] Ya.O. Mezhuev, Yu.V. Korshak, M.I. Shtil'man, Effect of poly(ethylene oxide) on the kinetics of oxidative polymerization of aniline, Russ. J. Gen. Chem. 86 (11) (2016) 2520–2525, https://doi.org/10.1134/S1070363216110190.
[27] Mukut Chakraborty, D.C. Mukherjee, Broja M. Mandal, Dispersion polymerization of aniline in different media: a UV−Visible spectroscopic and kinetic study, Langmuir 16 (6) (2000) 2482–2488, https://doi.org/10.1021/la990943d.
[28] Yoke Fong, Chengbo Chen, Joseph B. Schlenoff, In-situ monitoring of the kinetics and mechanism of conducting polymer synthesis, MRS Proc. 247 (1992) 693–698, https://doi.org/10.1557/proc-247-693.
[29] Yueping Fu, Ronald L. Elsenbaumer, Thermochemistry and kinetics of chemical polymerization of aniline determined by solution calorimetry, Chem. Mater. 6 (5) (1994) 671–677, https://doi.org/10.1021/cm00041a018.
[30] Ya.L. Kogan, G.I. Davidova, E.I. Knerelman, G.V. Gedrovich, L.S. Fokeeva, L. V. Emelina, V.I. Savchenko, Kinetic peculiarities of chemical aniline polymerization, Synth. Met. 41–43 (1991) 887–890, https://doi.org/10.1016/0379-6779(91)91519-G.
[31] Gordana Nestorovic, Katarina Jeremic, Slobodan Jovanovic, Kinetics of aniline polymerization initiated with iron(III) chloride, J. Serb. Chem. Soc. 71 (8–9) (2006) 895–904, https://doi.org/10.2298/JSC0609895N.
[32] S.M. Sayyah, A.A. Abd El-Khalek, A.A. Bahgat, H.M. Abd El-Salam, Kinetic studies of the polymerization of substituted aniline in aqueous solutions and characterization of the polymer obtained, Int. J. Polym. Mater. 49 (2001) 25–49, https://doi.org/10.1080/00914030108035865.
[33] Yen Wei, Kesyin F. Hsueh, Guang-Way Jang, Monitoring the chemical polymerization of aniline by open-circuit-potential measurements, Polymer 35 (16) (1994) 3572–3575, https://doi.org/10.1016/0032-3861(94)90927-x.
[34] V.I. Krinichnyi, Dynamics of spin charge carriers in polyaniline, Appl. Phys. Rev. 1 (2) (2014), 021305, https://doi.org/10.1063/1.4873329.
[35] A.V. Kulikov, V.R. Bogatyrenko, O.V. Belonogova, L.S. Fokeeva, A.V. Lebedev, T. A. Echmaeva, I.G. Shunina, ESR study of mechanism of polyaniline conductivity, Russ. Chem. Bull. Int. Ed. 51 (12) (2002) 2216–2223, https://doi.org/10.1023/a:1022127100633.
[36] K. Koziel, M. Lapkowski, E. Genies, ESR study of polyaniline doping at various concentrations of anions, Synth. Met. 84 (1997) 105–106, https://doi.org/10.1016/s0379-6779(96)03858-1.
[37] T. Ohsawa, O. Kimura, M. Onoda, K. Yoshino, An ESR study on polyaniline in nonaqueous electrolyte, Synth. Met. 47 (2) (1992) 151–156, https://doi.org/10.1016/0379-6779(92)90382-S.
[38] F. Yılmaz, Z. Küçükyavuz, Solution properties of polyaniline, Polym. Int. 59 (4) (2010) 552–556, https://doi.org/10.1002/pi.2736.
[39] S. Yalçınkaya, N. Çolak, Synthesis and characterization of poly(aniline-co-o-aminoaniline), Des. Monomers Polym. 15 (2) (2012) 147–157, https://doi.org/10.1163/156855511×615038.

[40] L. Ding, Q. Li, D. Zhou, H. Cui, R. Tang, J. Zhai, Copolymerization of aniline with m-nitroaniline and removal of m-nitroaniline from aqueous solutions using a polyaniline-modified electrode: a comparative study, Electrochim. Acta 77 (2012) 302–308, https://doi.org/10.1016/j.electacta.2012.06.012.

[41] H.S.O. Chan, S.C. Ng, W.S. Sim, K.L. Tan, B.T.G. Tan, Preparation and characterization of electrically conducting copolymers of aniline and anthranilic acid: evidence for self-doping by x-ray photoelectron spectroscopy, Macromolecules 25 (22) (1992) 6029–6034, https://doi.org/10.1021/ma00048a026.

[42] Haruo Matsuda, Kenji Osaki, Isamu Nitta, Crystal structure of quinhydrone, $C_{12}H_{10}O_4$, Bull. Chem. Soc. Jpn. 31 (5) (1958) 611–620, https://doi.org/10.1246/bcsj.31.611.

[43] T. Sakurai, The crystal structure of the triclinic modification of quinhydrone, Acta Cryst. 19 (3) (1965) 320–330, https://doi.org/10.1107/s0365110×65003390.

[44] A.O. Patil, W.T. Pennington, G.R. Desiraju, D.Y. Curtin, I.C. Paul, Recent studies on the formation and properties of quinhydrone complexes, Mol. Cryst. Liq. Cryst. 134 (1) (1986) 279–304, https://doi.org/10.1080/00268948608079591.

[45] Emily K. Golz, Vander Griend, A. Douglas, Modeling methylene blue aggregation in acidic solution to the limits of factor analysis, Anal. Chem. 85 (2) (2013) 1240–1246, https://doi.org/10.1021/ac303271m.

[46] E.N. Konyushenko, J. Stejskal, M. Trchová, N.V. Blinova, P. Holler, Polymerization of aniline in ice, Synth. Met. 158 (21–24) (2008) 927–933, https://doi.org/10.1016/j.synthmet.2008.06.015.

[47] V.I. Krinichnyi, A.L. Konkin, A.P. Monkman, Electron paramagnetic resonance study of spin centers related to charge transport in metallic polyaniline, Synth. Met. 162 (2012) 1147–1155, https://doi.org/10.1016/j.synthmet.2012.04.030.

[48] V.M. Kobryanskii, S.A. Arnautov, M.V. Motyakin, ESR investigation of water-soluble polyaniline formation, Synth. Met. 69 (1995) 221–222.

[49] Victor I. Krinichnyi, 292 c. Multi Frequency EPR Spectroscopy of Conjugated Polymers and Their Nanocomposites, CRC Press, Boca Raton, 2017. ISBN 978-1-4987-7964-7.

[50] A.V. Kulikov, Ya.L. Kogan, L.S. Fokeeva, Study of growth of polyaniline chain by EPR method, Synth. Met. 55–57 (1993) 1023–1028.